
GSVC: EFFICIENT VIDEO REPRESENTATION AND COMPRESSION THROUGH 2D GAUSSIAN SPLATTING

A PREPRINT

Longan Wang

Yuang Shi

Wei Tsang Ooi

Department of Computer Science
National University of Singapore
Singapore

{wanglongan,yuangshi,ooiwt}@comp.nus.edu.sg

<https://yuang-ian.github.io/gsvc/>

January 23, 2025

ABSTRACT

3D Gaussian splats have emerged as a revolutionary, effective, learned representation for static 3D scenes. This work explores 2D Gaussian splats as a new primitive for representing videos. We propose GSVC, an approach to learning a set of 2D Gaussian splats that can effectively represent and compress video frames. GSVC incorporates the following techniques: (i) To exploit temporal redundancy among adjacent frames, which can speed up training and improve the compression efficiency, we predict the Gaussian splats of a frame based on its previous frame. (ii) To control the trade-offs between file size and quality, we remove Gaussian splats with low contribution to the video quality; (iii) To capture dynamics in videos, we randomly add Gaussian splats to fit content with large motion or newly-appeared objects; (iv) To handle significant changes in the scene, we detect key frames based on loss differences during the learning process. Experiment results show that GSVC achieves good rate-distortion trade-offs, comparable to state-of-the-art video codecs such as AV1 and HEVC, and a rendering speed of 1500 fps for a 1920×1080 video.

1 Introduction

Signal processing techniques, particularly, frequency domain signals, serve as the basis for current digital video coding standards [Wiegand et al.(2003), Sullivan et al.(2012), Sullivan(2020)]. Neural-based approaches (e.g., [Li et al.(2023), Li et al.(2024)]), driven by recent advances in deep learning, provide a promising alternative by learning a data-driven implicit representation that can adapt to diverse video characteristics. However, neural-based approaches often require large amounts of memory and high computational cost. Furthermore, to be widely adopted in practice, a video encoder should support various “knobs” to control trade-offs between encoding quality, compression rate, and encoding time, and to support diverse inputs (e.g. resolutions, amount of motion) and application context (e.g. variable bitrate, low-latency encoding, scalable encoding, random access). Supporting all these features, which are already mature and widely used in current video coding standards, remains a challenge for neural-based video encoders.

Recently, 3D Gaussian Splatting (3DGS) [Kerbl et al.(2023)], first proposed in 2023, has revolutionized visual data representation for 3D scenes. Unlike neural-based implicit representations, such as Neural Radiance Field (NeRF) [Mildenhall et al.(2021)], 3DGS learns explicit Gaussian splats as primitives to represent a 3D scene in high quality. Using a differentiable tile-based rasterization framework, 3DGS allows the captured scene to be rendered quickly.

Given the emergence of Gaussian splats, our work in this paper seeks to answer a question: “*Can Gaussian splats be used as an effective alternative representation for digital video compression?*”

Two recent work, VGR [Sun et al.(2024)] and VeGaS [Smolak-Dyżewska et al.(2024)] have applied 3DGS for representing 2D videos. They are not designed with compression as the main goal. On the other hand, 2D Gaussian splat (2DGS) [Zhang et al.(2025), Zhang et al.(2024)] has been proposed as a primitive for image representation. Representing visual data using 2D Gaussian splats requires fewer attributes, and thus is more storage efficient compared to 3D Gaussian splats. The rendering process is more natural since depth computation is not needed for 2D images.

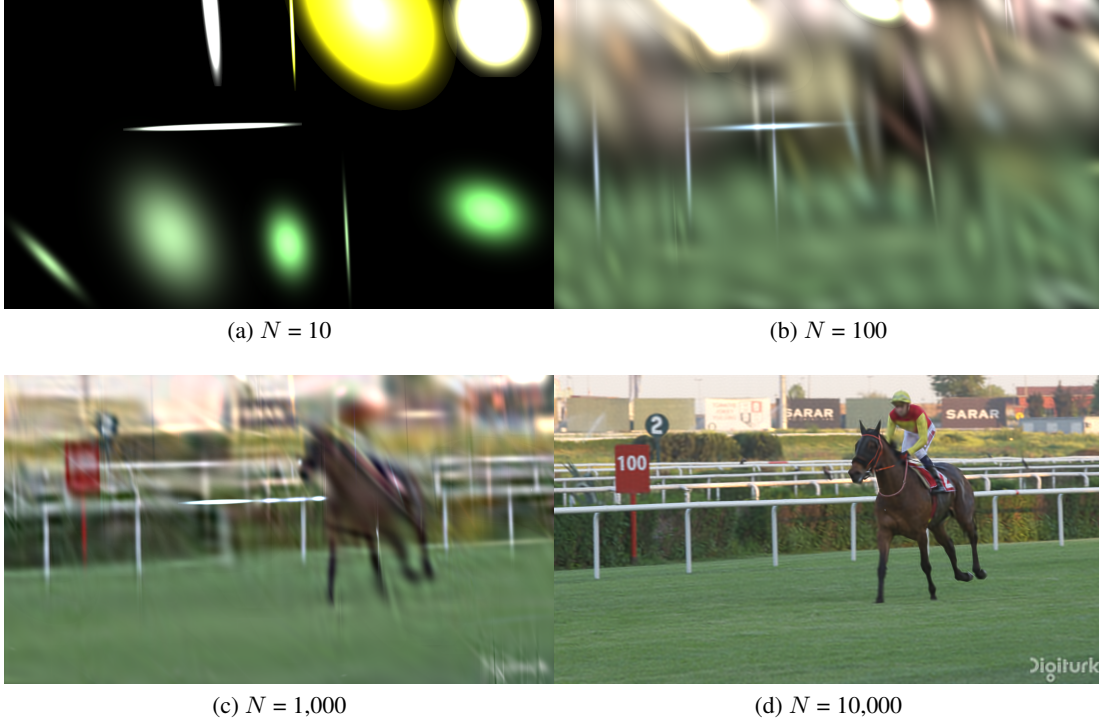


Figure 1: Using Gaussian splats to model an image. Image is taken from UVG *Jockey* video. The sub-figures show that as the number of Gaussian splats N increase, the learned splats increasing approximates the image’s content

Figure 1 and Figure 2 illustrate how Gaussian splats can serve as a primitive for representing an image, and how the training process iteratively optimizes the parameters of the Gaussian splats to fit a given image.

While 2D Gaussian splat has been shown to be an effective representation of images, extending it to dynamic video representation poses new challenges. Video representation requires consideration of temporal coherence and dynamics in the video, which 2DGS does not address.

To tackle the challenges above, we propose a novel video representation and compression framework termed GSVC based on 2D Gaussian splats. Similar to modern video codecs, GSVC categorizes video frames into key-frames (I-frame) and predicted frames (P-frames). Gaussian splats representation for the I-frame is learned from scratch while, for P-frames, it is learned incrementally from its previous frame. The predicted frames allow us to exploit temporal redundancy among the frames. To allow rate control to trade off between compression rate and quality, GSVC prunes Gaussian splats with low contributions to the frame quality. To cater to video dynamics, GSVC augments each P-frame with random splats before optimization. Finally, we monitor the loss values when learning the splats of each frame to determine if a frame should be an I-frame or a P-frame. This step allows GSVC to detect significant changes in the scene.

The main contributions of GSVC are summarized as follows:

- We demonstrate the efficacy of 2D Gaussian splats as a new primitive for representing video frames for compression.
- We address the challenges of learning Gaussian splats for video representation using several techniques: incremental learning, Gaussian splats pruning, Gaussian splats augmentation, and key-frame identification. With these techniques, our approach enables a compact representation while effectively capturing abrupt objects, large deformations, and scene transitions.

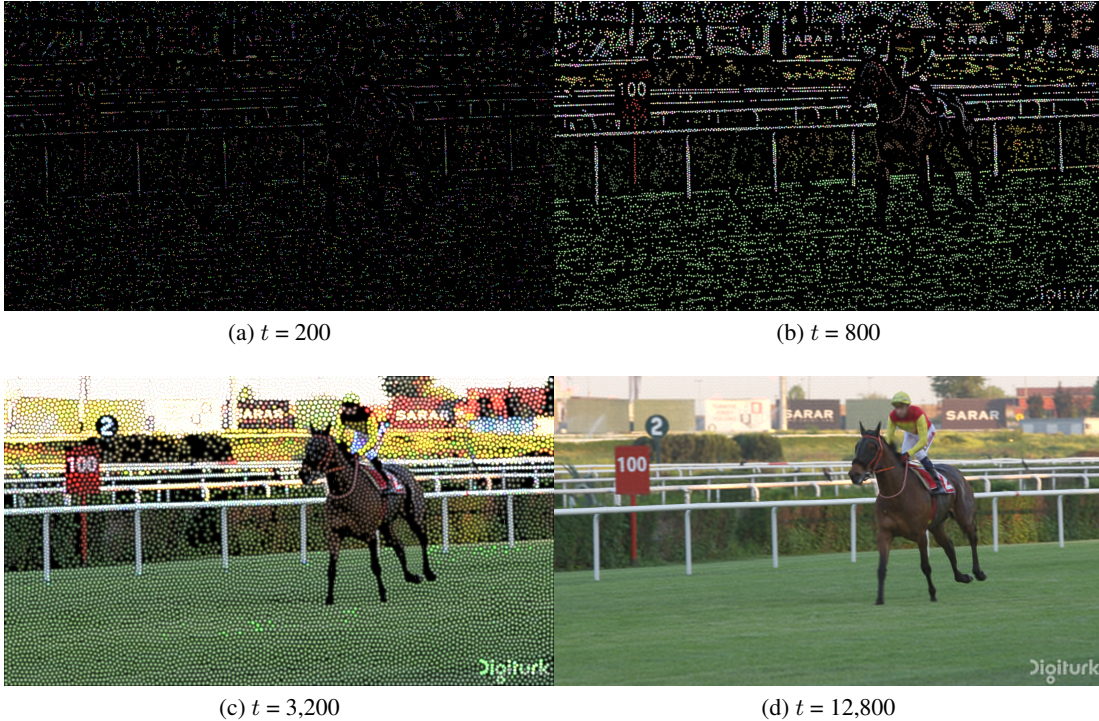


Figure 2: Image taken from UVG *Jockey* video. Intermediate training results after t iterations for 10,000 Gaussian splats, illustrating how Gaussian splats parameters are optimized to fit the content of a frame.

- We present experiment results, demonstrating that GSVC achieves a rate-distortion performance comparable to state-of-the-art video compression standards while allowing fast decoding speeds of up to 1500 FPS.

2 Related Work

Signal processing techniques, particularly frequency-domain representations, form the foundation of modern video compression standards such as AVC [Wiegand et al.(2003)], HEVC [Sullivan et al.(2012)], and VVC [Sullivan(2020)]. These standards rely on hand-crafted modules like block-based motion compensation and Discrete Cosine Transform (DCT) to achieve efficient compression [Lu et al.(2019)]. Much research, development, and standardization effort has gone into these video compression standards in the last 35 years. While great strides are still being made in improving the codecs and new standards are still being proposed, the community is also exploring new approaches to compress digital videos.

Recent advances in neural-based approaches provide a promising alternative to traditional standards [Li et al.(2022), Li et al.(2023)]. By leveraging deep learning to jointly optimize the whole compression system, these methods learn data-driven representations that adapt flexibly to varying video characteristics [Lu et al.(2019)]. Despite their potential, these approaches face significant challenges: decoding is computationally expensive, and their implicit neural representations hinder direct editing and processing.

Recent efforts have explored Gaussian-based representations for video compression through explicit Gaussian primitives. VGR [Sun et al.(2024)] models each frame using 3D Gaussian splats as if representing a static 3D scene, while VeGaS [Smolak-Dyżewska et al.(2024)] treats video sequences as 3D data with time as the third dimension. However, both methods are constrained by the static nature of 3DGS, leading to inefficiencies such as large model sizes and limited flexibility in capturing the dynamic and spatiotemporal complexities inherent in video content.

Recent efforts have explored Gaussian-based representations for video compression through explicit Gaussian primitives. VGR [Sun et al.(2024)] models each frame using 3D Gaussian splats as if representing a static 3D scene, while VeGaS [Smolak-Dyżewska et al.(2024)] treats video sequences as 3D data with time as the third dimension. However, both methods are constrained by the static nature of 3DGS, leading to inefficiencies such as large model sizes and limited flexibility in capturing the dynamic and spatiotemporal complexities inherent in video content.

3 GSVC

We begin by formulating the problem in Section 3.1, followed by an in-depth discussion on the structure and rendering of 2D Gaussian splats in Section 3.2. We then present the mechanism for frame prediction in Section 3.3. Then, in Section 3.4, we describe how GSVC removes Gaussian splats to reduce the size with minimal impact on the quality. In Section 3.5, we introduce GSA, designed to add new Gaussian splats, accommodating large deformations and abrupt objects. Section 3.6 provides the details for DKS, a method that dynamically selects key-frames to prevent unrelated scene priors from affecting model performance. Finally, we integrate all components to illustrate the complete training pipeline in Section 3.7 and detail the encoding strategy in Section 3.8.

3.1 Problem Formulation

We first introduce the notations for our video encoding pipeline. Let $\mathcal{F} = \{f_1, f_2, \dots, f_T\}$ denote a video with T frames. Our objective is to encode it as $\widehat{\mathcal{F}} = \{\widehat{f}_1, \widehat{f}_2, \dots, \widehat{f}_T\}$. In $\widehat{\mathcal{F}}$, each frame \widehat{f}_t is represented by a set of 2D Gaussian splats $\mathcal{G}_t = \{\mathbf{G}_{t,1}, \mathbf{G}_{t,2}, \dots, \mathbf{G}_{t,N_t}\}$, where N_t is the number of Gaussian splats in f_t . To maintain consistency, we set $N_t = N$ for all f_t . The number of Gaussian splats per frame N serves as a *rate control* parameter to tune the tradeoff between quality and size.

The entire video can be expressed as:

$$\mathcal{G} = \{\mathcal{G}_1, \mathcal{G}_2, \dots, \mathcal{G}_T\}, \quad (1)$$

3.2 2D Gaussian Image Representation

To achieve an efficient Gaussian representation, it is essential to maintain a compact and flexible Gaussian Splat structure. Driven to achieve this goal and informed by the proven success of 2DGS [Zhang et al.(2025), Zhang et al.(2024)], we adopt a similar parameterization and rendering approach. Each 2D Gaussian splat is characterized by three attributes, comprising a total of eight parameters: position $\boldsymbol{\mu} \in \mathbb{R}^2$, weighted color $\mathbf{c}' \in \mathbb{R}^3$, and Cholesky vector $\boldsymbol{\ell} \in \mathbb{R}^3$. Specifically, the weighted color \mathbf{c}' is formed by integrating the opacity $o \in \mathbb{R}$ into the color coefficients $\mathbf{c} \in \mathbb{R}^3$. The Cholesky vector $\boldsymbol{\ell} = \{\ell_1, \ell_2, \ell_3\}$ represents the lower triangular elements of the matrix \mathbf{L} , which describes the covariance matrix $\boldsymbol{\Sigma} \in \mathbb{R}^{2 \times 2}$ using the Cholesky decomposition [Higham(2009)]:

$$\boldsymbol{\Sigma} = \mathbf{L}\mathbf{L}^T. \quad (2)$$

This decomposition ensures the covariance matrix remains positive semi-definite during optimization, preventing invalid parameter updates.

At a high level, the training process works as follows (the details and complete pipeline will be given in Section 3.7). Given an input RGB image F_t , we repeatedly optimize the number of Gaussians and their parameters so that the set of Gaussian splats G_t when rendered, approximates F_t as much as possible.

For rendering, the color C_i at the i -th pixel is computed using an accumulated summation mechanism based on \mathbf{c}' . The formulation is defined as:

$$C_i = \sum_{n \in \mathcal{N}} \mathbf{c}'_n \cdot \exp(-\sigma_n), \quad (3)$$

where \mathcal{N} represents the number of Gaussian splats covering the i -th pixel. Additionally, σ_n is defined as follows:

$$\sigma_n = \frac{1}{2} \mathbf{d}_n^T \boldsymbol{\Sigma}^{-1} \mathbf{d}_n, \quad (4)$$

where \mathbf{d}_n denotes the distance between the pixel center and the projected Gaussian center.

3.3 Frame Prediction

A naive approach towards representing a video with Gaussian splats is to represent each frame as an image independently (e.g., each frame is a GaussianImage [Zhang et al.(2025)]). Doing so is analogous to encoding a video as a Motion JPEG or an I-frame-only MPEG video. However, we can exploit temporal redundancy in a video to improve encoding (*i.e.*, training) speed and encoding efficiency.

Similar to modern video encoders, GSVC designates selected frames as key-frames (or I-frames). The selection of key-frames is presented in Section 3.6. A key-frame is trained from scratch, independently of any previous frames. The set of Gaussian splats is initialized from random parameters.

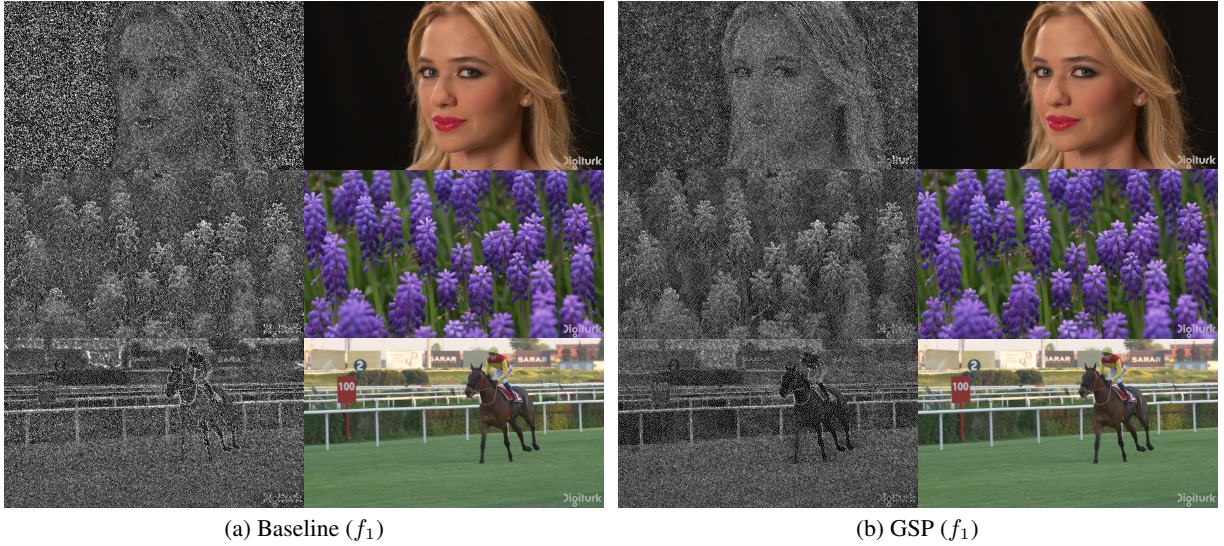


Figure 3: Distribution of Gaussian Splat Centers (45K) on f_1 in *Beauty*, *HoneyBee* and *Jockey*.

Non-key-frames are then predicted from the previous frames. Borrowing the terms from modern video encoders, we call these the P-frames. During training, the Gaussian splats from the previous frame are used for initialization. The parameters of these Gaussians are thus fine-tuned to fit the current frame. Only the differences between the parameters of the Gaussian splats between the previous and the current frames are stored.

We extend our notations above with a superscript to denote a frame as either an I-frame or a P-frame, using \mathcal{G}_t^I and \mathcal{G}_t^P respectively.

3.4 Gaussian Splat Pruning

A key step in video encoding is to tune the trade-off between the encoding rate and the quality. For constant bitrate encoding, the encoder attempts to maintain a constant bitrate through the video but allows the quality to vary. In our context, constant bitrate is achieved by keeping the same number of Gaussian splats N for every frame. On the other hand, for constant quality encoding, the encoder keeps the frame quality constant but allows the bitrate to vary. In GSVC, this corresponds to removing Gaussian splats during the training process, while keeping the frame quality above a threshold.

For either approach above, a critical step is to remove Gaussian splats with minimal impact on the image quality. We introduce Gaussian Splat Pruning (GSP) to achieve this. Specifically, we introduce a learnable parameter w to record the contribution of each Gaussian splat during the rendering process during training, based on their weighted color c' . Accordingly, the rendering formula in Equation (3) is modified as follows:

$$C_i = \sum_{n \in \mathcal{N}} w_n c'_n \cdot \exp(-\sigma_n), \quad (5)$$

where w_n represents the importance of the n -th Gaussian. By keeping Gaussian splats with high $|w_n|_2$ values, we can eliminate those with lower contributions, reducing the number of splats while preserving the quality of the video representation as much as possible.

Note that the parameter w is not passed to subsequent P-frames \mathcal{G}_{t+1}^P to avoid increasing the model size. Instead, the product $w c'$ in \mathcal{G}_t^* is used to initialize the weighted color coefficient c' in \mathcal{G}_{t+1}^P , ensuring an efficient and compact representation across frames.

Figure 3 demonstrates the impact of the GSP. The figures depict the center of the Gaussian splats and the corresponding rendered images taken from Frame 1 of the dataset. The figures contain 45,000 Gaussians. The left figures show the baseline approach where we optimized 45,000 Gaussian splats without pruning. The right figures illustrate the impact of GSP. We initialized the training process with 50,000 Gaussians and pruned 5,000 away during training. The results show that the remaining Gaussian splats, after GSP, are more concentrated towards regions of the image with higher details, allowing GSVC to capture the details of the images.

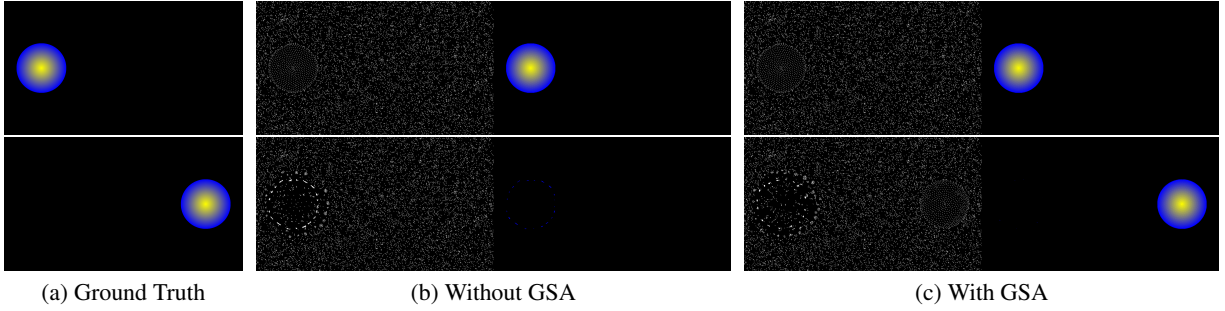


Figure 4: Distribution of Gaussian Splats (45k) on f_5 in *Beauty*.

3.5 Dynamic Content

During training, the Gaussian splats of P-frames adapt their parameters to changes from the previous frames. This approach, however, can fail to capture highly dynamic content. For example, a new object not in the previous frame may appear in the current frame; the current frame contains high motion. Such dynamics may cause challenges to the training process, leading to lower frame quality.

To address this, we propose Gaussian Splat Augmentation (GSA), which introduces new Gaussian splats to better handle dynamics in the frames. Specifically, in each P-frame, after initialization using results from the previous frame, every Gaussian splat’s contribution w is set to 1. New Gaussian splats with w set close to zero are then added uniformly and randomly to the frame. During training, we again apply GSP to remove Gaussian splats with low contribution. This strategy ensures that new Gaussian splats placed over new or dynamic content can be easily activated during training, due to sharp changes in w , allowing them to learn and capture the dynamics effectively. At the same time, splats in well-represented regions with minimal changes in w will be as removed by GSP.

Therefore, by coordinating GSA and GSP, our framework can adapt to dynamic content while exploiting temporal redundancy in P-frames. These augmented Gaussian splats are analogous to intra-coded macroblocks in P-Frames, in standard video codecs.

Figure 4 illustrates the impact of the GSA using two frames from a synthetic video (4(a)), depicting a circle that jumps from the left of the image to the right in the next frame. The figures 4(b) and (c) depict the distribution of the position of Gaussian splats and their corresponding rendered images without GSA and with GSA, respectively. Without GSA, the predicted Gaussian splats are stuck in a local minimum and are not able to converge to a set of parameters that capture the new position of the circle, resulting in an empty frame. On the other hand, GSA allows the augmented Gaussians to capture the new position of the circle.

3.6 Scene Transition Detection

While GSA can adapt effectively to frame content dynamics, its effectiveness decreases as the changes across frames become more drastic. Even if the augmented Gaussian splats can capture the changes, as the differences between the two frames increase, the compression efficiency decreases. Thus, it is more effective to insert a key-frame when there is a significant difference between two adjacent frames, such as when there is a scene change.

We propose a Dynamic Key-frame Selector (DKS) method to identify significant frame differences. The proposed DKS detects scene transitions by analyzing the loss differences between key-frame and P-frame pre-training. Each frame f_t in the video $\mathcal{F} = \{f_1, f_2, \dots, f_T\}$ is first trained as a key-frame, yielding a set of loss values:

$$\ell^I = \{\ell_1^I, \ell_2^I, \dots, \ell_T^I\}. \quad (6)$$

Subsequently, each frame (except the first) is pre-trained as a P-frame, resulting in another set of loss values:

$$\ell^P = \{\ell_2^P, \ell_3^P, \dots, \ell_T^P\}. \quad (7)$$

The loss differences are computed as:

$$\Delta\ell = \{\Delta\ell_t \mid \Delta\ell_t = \ell_t^P - \ell_t^I, \quad t = 2, \dots, T\}. \quad (8)$$

To detect scene transitions, we identify outliers in $\Delta\ell$ by modeling its local distribution using a sliding window. A frame f_t is classified as a scene transition if its loss difference $\Delta\ell_t$ exceeds the local mean μ_t by more than three times

Algorithm 1 GSVC Training Pipeline

Require: Video frames $\mathcal{F} = \{f_1, f_2, \dots, f_T\}$, Gaussian splats \mathcal{G} ;

- 1: Pre-train each frame from scratch to get \mathcal{G}^I and compute ℓ^I ;
- 2: Pre-train each frame as \mathcal{G}^P according to \mathcal{G}^I and compute ℓ^P ;
- 3: Select key-frames to get \mathcal{I} according to Equation (12);
- 4: **for** $t \in \{1, 2, \dots, T\}$ **do**
- 5: **if** $f_t \in \mathcal{I}$ **then**
- 6: Initialize \mathcal{G}_t^* as \mathcal{G}_t^I randomly;
- 7: **else**
- 8: Initialize \mathcal{G}_t^* as \mathcal{G}_t^P according to \mathcal{G}_{t-1}^* and inject splats;
- 9: **end if**
- 10: **while** not converge **do**
- 11: Remove redundant splats according to w in Equation (3);
- 12: Update parameters according to Equation (13);
- 13: **end while**
- 14: **end for**

Ensure: Optimized Gaussian splats $\mathcal{G} = \{\mathcal{G}_1^I, \mathcal{G}_2^*, \dots, \mathcal{G}_T^*\}$.

the local standard deviation σ_t :

$$\Delta \ell_t > \mu_t + 3\sigma_t, \quad (9)$$

where the local mean μ_t and standard deviation σ_t are calculated within a window \mathcal{W}_t centered around t :

$$\mu_t = \frac{1}{|\mathcal{W}_t|} \sum_{i \in \mathcal{W}_t} \Delta \ell_i, \quad \sigma_t = \sqrt{\frac{1}{|\mathcal{W}_t|} \sum_{i \in \mathcal{W}_t} (\Delta \ell_i - \mu_t)^2}. \quad (10)$$

The window \mathcal{W}_t is defined as:

$$\mathcal{W}_t = \{\Delta \ell_i \mid \max(2, t - w_{\text{win}}) \leq i \leq \min(T, t + w_{\text{win}})\}, \quad (11)$$

where w_{win} is the window size. The key-frame set \mathcal{I} is constructed by including the first frame and all frames identified as scene transitions:

$$\mathcal{I} = \{1\} \cup \{t \mid \Delta \ell_t > \mu_t + 3\sigma_t, t = 2, \dots, T\}. \quad (12)$$

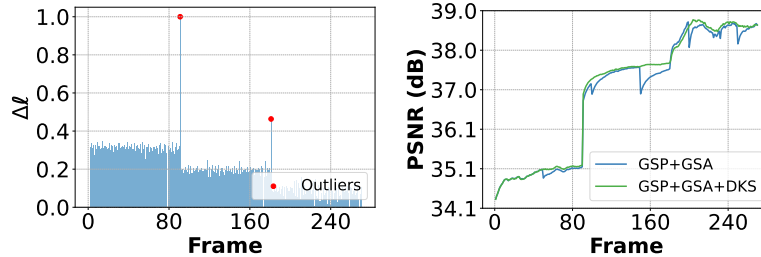


Figure 5: $\Delta \ell$ and PSNR over frames on the concatenated videos.

Figure 5 demonstrate the process and key-frame selection. We synthesize a video by concatenating the first 90 frames of *Beauty*, *HoneyBee*, and *Jockey* from the UVG dataset into one video. The graph on the left plots the changes in loss $\delta \ell_t$ across frames. We can see two spikes, corresponding to the outliers during scene change (seams when two videos are concatenated). The plot on the right shows the PSNR of individual frames, comparing when we employ DSK to dynamically decide the key-frames versus when we do not use DSK. In the latter case, we insert a key-frame periodically every 50 frames. The plot shows that inserting a key-frame when there is no scene change is detrimental to the frame quality (there is a slight drop in PSNR every 50 frames) since GSVC learns the splats from scratch.

3.7 Putting Everything Together

We now explain how we combine all four mechanisms above into the training process of GSVC. Following Zhang *et al.* [Zhang et al.(2025)], we utilize the L2 loss function to minimize the distortion between each original frame $f_t \in \mathcal{F}$

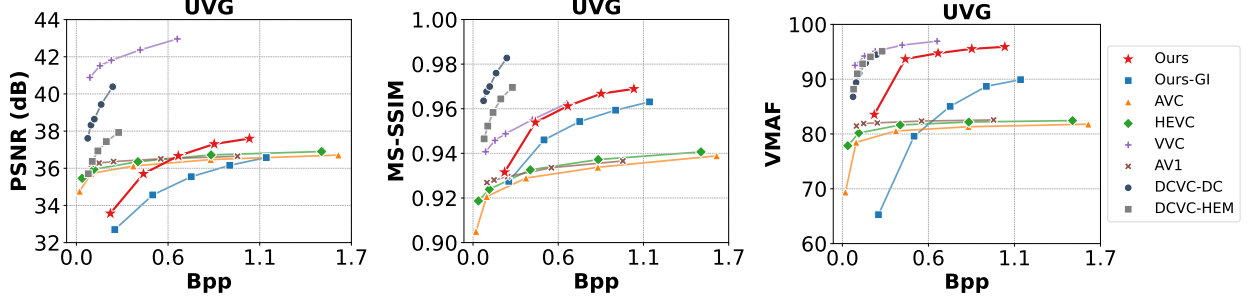


Figure 6: Rate-Distortion Curves in PSNR, MS-SSIM and VMAF: comparison of our approach with baselines

and its reconstructed frame $\hat{f}_t \in \hat{\mathcal{F}}$. The L2 loss function on f_t is given as:

$$\mathcal{L}_2^t = \frac{1}{H \times W} \sum_{i=1}^H \sum_{j=1}^W \left\| f_t(i, j) - \hat{f}_t(i, j) \right\|_2^2, \quad (13)$$

where H and W are the height and width of the frame (in pixels), $f_t(i, j)$ and $\hat{f}_t(i, j)$ denote the original and reconstructed pixel intensities at position (i, j) in f_t and \hat{f}_t , respectively. The training process of our GSVC on video representation is shown in Algorithm 1.

3.8 Encoding

The process above learns the representation of a video as a set of Gaussian splats \mathcal{G} . To efficiently encode \mathcal{G} , we employ a temporal-aware fine-tuning strategy tailored for videos, producing $\hat{\mathcal{G}}$. For each frame f_i , its n -th Gaussian splat $\mathcal{G}_{i,n} = \{\mu_n, \ell_n, \mathbf{c}'_n\}$ is encoded as:

$$\hat{\mathcal{G}}_{i,n} = \begin{cases} \mathcal{Q}(\mathcal{G}_{i,n}), & \text{if } \mathcal{G}_i^I, \\ \mathcal{Q}(\Delta\mathcal{G}_{i,n}) + \mathcal{G}_{i-1,n}, & \text{if } \mathcal{G}_i^P, \end{cases} \quad (14)$$

$$\Delta\mathcal{G}_{i,n} = \{\mu_n - \mu_{n-1}, \ell_n - \ell_{n-1}, \mathbf{c}'_n - \mathbf{c}'_{n-1}\},$$

where, $\mathcal{Q}(\cdot) = \{\mathcal{Q}_\mu(\cdot), \mathcal{Q}_\ell(\cdot), \mathcal{Q}_c(\cdot)\}$ denotes the quantization operator based on the Attribute Quantization-aware Fine-tuning [Zhang et al.(2025)] designed for 2D Gaussian splats. Specifically, For position μ , 16-bit float precision is used as $\mathcal{Q}_\mu(\mu)$. For the Cholesky vector ℓ , b-bit asymmetric quantization [Bhalgat et al.(2020)] is applied:

$$\mathcal{Q}_\ell(\ell_i) = \hat{\ell}_i \times \gamma_i + \beta_i$$

$$\hat{\ell}_i = \left\lceil \text{clamp} \left(\frac{\ell_i - \beta_i}{\gamma_i}, 0, 2^b - 1 \right) \right\rceil, \quad (15)$$

where $i \in \{0, 1, 2\}$, and γ_i, β_i are learned scaling and offset factors. For weighted color \mathbf{c} , residual vector quantization [Zeghidour et al.(2021)] cascades M stages of VQ [Gray(1984)] with codebook size B :

$$\mathcal{Q}_c(\mathbf{c}') = \sum_{k=1}^M \mathbf{C}^k [i^k],$$

$$i^k = \arg \min_k \left\| \mathbf{C}^k [i^k] - \left(\mathbf{c}' - \sum_{j=1}^{k-1} \mathbf{C}^j [i^j] \right) \right\|_2^2, \quad (16)$$

where $\mathbf{C}^k \in \mathbb{R}^{B \times 3}$ is the k -th stage codebook, and i^k is the codebook index. The codebooks are trained with the commitment loss [Zhang et al.(2025)].

4 Experiments

4.1 Experimental Setup

Datasets. We evaluate our method on the UVG Dataset [Mercat et al.(2020)], selecting three representative videos (e.g. *Beauty*, *HoneyBee*, and *Jockey*), representing slow, medium, and fast motion, respectively. Each video consists of 600 frames. All videos are standardized to 1920×1080 resolution, 120 fps, 4:2:0 chroma subsampling, 8-bit depth, and YUV color space.

Evaluation Metrics. We evaluate our method using three widely adopted metrics: Peak Signal-to-Noise Ratio (PSNR), Multi-Scale Structural Similarity Index Measure (MS-SSIM) [Wang et al.(2003)], and Video Multi-Method Assessment Fusion (VMAF) [Netflix(2023)]. PSNR quantifies reconstruction fidelity in decibels (dB) by comparing the maximum signal power to noise. MS-SSIM measures perceptual similarity based on luminance, contrast, and structure across multiple scales, with values ranging from 0 to 1, where higher indicates better similarity. VMAF combines human visual perception models to provide a comprehensive assessment of video quality, offering a score from 0 to 100, where higher scores denote better quality.

Implementation Details. Our GSVC framework is built on the gsplat library [Ye et al.(2024)] and utilizes CUDA-based rasterization optimized with accumulated blending [Zhang et al.(2025)]. Gaussian parameters are optimized using the Adan optimizer [Xie et al.(2024)] with an initial learning rate of $1e^{-3}$, halved every 20,000 steps. Pre-training is performed with 500 iterations for both key-frames and P-frames. The window size w_{win} is set to 10. key-frames apply GSP to remove 10% of the initial N splats. To maintain a consistent total of N Gaussian splats per frame, each P-frame begins with the inherited reduced set (*i.e.* 90% of N) from the preceding frame. GSA then adds 10% new Gaussian splats. After training, GSP prunes 10% of the splats, bringing the total back to 90% of N . All experiments are carried out on NVIDIA V100 GPUs using PyTorch [Paszke et al.(2019)]. We train the models for 50K iterations, or until the model has converged. The convergence is defined as 100 consecutive iterations with at most $1e^{-7}$ changes in the L_2 loss between two iterations. We use constant-rate coding for our experiments, ranging N from 10, 000 to 50, 000 with a 10, 000 increment.

Baseline. We compare against three groups of existing methods. First, we benchmark against standard video codecs, including H.264/AVC [Wiegand et al.(2003)], H.265/HEVC [Sullivan et al.(2012)], H.266/VVC [Sullivan(2020)], and AV1 [Chen et al.(2020)]. For AVC, HEVC, and AV1, we use the ffmpeg implementation (version 5.1), varying the CRF (`--crf`) parameter from 30 to 10 to assess compression quality. For VVC, we use VVCSoftware_VTM (version 23.6) in random-access mode with the QP (`--QP`) parameter adjusted from 28 to 18. Default encoding parameters are used unless otherwise specified to ensure consistency across evaluations. Second, we compare our methods against two recent neural video compression methods, DCVC-HEM [Li et al.(2022)] and DCVC-DC [Li et al.(2023)]. Finally, we use GaussianImage [Zhang et al.(2025)] to encode each frame independently, as a baseline for a naive Gaussian splats-based video representation. We denote this as Ours-GI in the experiments below. We did not compare them with the 3DGS methods as they are designed to support video editing rather than compression, and thus their size are not comparable.

4.2 Comparison Analysis

Rate-Distortion Trade-off. Figure 6 presents the key results, showing GSVC’s rate-distortion curves and other baselines. We first note that we can achieve a significant improvement over Ours-GI – the I-frame only, GaussianImage approach, demonstrating the contributions of predictive frames, pruning, augmentation, and key-frame detections brought to the representation.

Next, we note that the neural-based approach achieves significant improvements over GaussianVideos and even some state-of-the-art codecs such as VVC in terms of MS-SSIM. These neural-based approaches, however, are pre-trained on the UVG dataset, and thus the superior performance is not surprising. The standard MPEG/H26x video codec and GSVC do not require any pre-training and can generalize well to any video.

Against the standardized video codec, GSVC achieves better or comparable performance in terms of MS-SSIM and VMAF (which consider image structure and human perception) except VVC. Our experiments on GSVC yield a lower PSNR – in certain scenarios. But, it is important to note that we use L_2 as a loss function, and we can tune the convergence condition to further improve the PSNR, without increasing N , if we sacrifice the encoding time.

Computational Cost. On the UVG dataset, the encoding time of our proposed GSVC method ranges from 197.58 seconds to 221.45 seconds per frame as the bit-per-pixel (bpp) increases from 0.2103 to 1.0715. GSVC can decode at the speed of 1583.72 fps. In contrast, the neural-based method DCVC-DC decodes at the speed of 2.4 fps. This superiority in decoding time is consistent with a key advantage of Gaussian splats reported in the literature [Kerbl et al.(2023), Zhang et al.(2025)].

4.3 Ablation Study

To analyze the contribution of each component in GSVC, we first compare GSVC against its three variants: (1) with P-frames only, (2) with P-frames and GSP, and (3) with P-frames, GSP and GSA. All comparative variants are trained using the same configurations. The results demonstrate that GSP contributes the most to the effectiveness of GSVC,

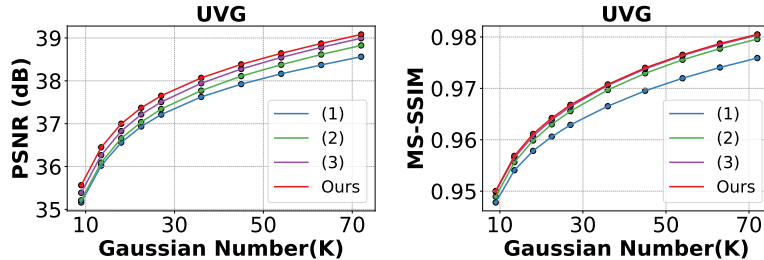


Figure 7: Ablation Study of PSNR and MS-SSIM over Gaussian Number on UVG dataset.

followed by GSA, and DSK. Particularly, we see that DSK has small improvements in terms of MS-SSIM, likely because there is no major scene change within each video in the UVG data we used.

5 Discussion and Conclusion

We present a new primitive, 2D Gaussian splats, as an alternative representation for video. By optimizing the parameters of the splats, we can achieve comparable rate-distortion performance with most of the widely used implementations of modern video codecs. Unlike neural-based approaches, Gaussian splat representation is explicit, and the training parameters allow us to directly control the size (number of Gaussian splats), quality (convergence threshold of the loss function), and encoding time (number of training iterations). Furthermore, it can naturally adapt to different resolutions and support fine-grain progressive coding (by adding back the pruned Gaussian splats).

The GSVC presented here is relatively simple and has yet to incorporate more complex compression techniques used in 3DGS. Furthermore, there is room for hyperparameter tuning to further improve GSVC. Additional techniques such as bidirectional predictions could also be integrated to further improve GSVC. Regardless, our results here serve as preliminary support of evidence on the efficacy of Gaussian splats as a viable alternative representation for video.

References

- [Bhalgat et al.(2020)] Yash Bhalgat, Jinwon Lee, Markus Nagel, Tijmen Blankevoort, and Nojun Kwak. 2020. LSQ+: Improving low-bit quantization through learnable offsets and better initialization. In *Proceedings of the IEEE/CVF conference on computer vision and pattern recognition workshops*. 696–697.
- [Chen et al.(2020)] Yue Chen, Debargha Mukherjee, Jingning Han, Adrian Grange, Yaowu Xu, Sarah Parker, Cheng Chen, Hui Su, Urvang Joshi, Ching-Han Chiang, et al. 2020. An overview of coding tools in AV1: the first video codec from the alliance for open media. *APSIPA Transactions on Signal and Information Processing* 9 (2020), e6.
- [Gray(1984)] Robert Gray. 1984. Vector quantization. *IEEE Assp Magazine* 1, 2 (1984), 4–29.
- [Higham(2009)] Nicholas J Higham. 2009. Cholesky factorization. *Wiley interdisciplinary reviews: computational statistics* 1, 2 (2009), 251–254.
- [Kerbl et al.(2023)] Bernhard Kerbl, Georgios Kopanas, Thomas Leimkühler, and George Drettakis. 2023. 3D Gaussian Splatting for Real-Time Radiance Field Rendering. *ACM Trans. Graph.* 42, 4 (2023), 139–1.
- [Li et al.(2022)] Jiahao Li, Bin Li, and Yan Lu. 2022. Hybrid Spatial-Temporal Entropy Modelling for Neural Video Compression. In *Proceedings of the 30th ACM International Conference on Multimedia*.
- [Li et al.(2023)] Jiahao Li, Bin Li, and Yan Lu. 2023. Neural Video Compression with Diverse Contexts. In *IEEE/CVF Conference on Computer Vision and Pattern Recognition, CVPR 2023, Vancouver, Canada, June 18-22, 2023*.
- [Li et al.(2024)] Jiahao Li, Bin Li, and Yan Lu. 2024. Neural video compression with feature modulation. In *Proceedings of the IEEE/CVF Conference on Computer Vision and Pattern Recognition*. 26099–26108.
- [Lu et al.(2019)] Guo Lu, Wanli Ouyang, Dong Xu, Xiaoyun Zhang, Chunlei Cai, and Zhiyong Gao. 2019. DVC: An end-to-end deep video compression framework. In *Proceedings of the IEEE/CVF conference on computer vision and pattern recognition*. 11006–11015.
- [Mercat et al.(2020)] Alexandre Mercat, Marko Viitanen, and Jarno Vanne. 2020. UVG dataset: 50/120fps 4K sequences for video codec analysis and development. In *Proceedings of the 11th ACM Multimedia Systems Conference*. 297–302.

- [Mildenhall et al.(2021)] Ben Mildenhall, Pratul P Srinivasan, Matthew Tancik, Jonathan T Barron, Ravi Ramamoorthi, and Ren Ng. 2021. NeRF: Representing scenes as neural radiance fields for view synthesis. *Commun. ACM* 65, 1 (2021), 99–106.
- [Netflix(2023)] Netflix. 2023. VMAF - Video Multi-Method Assessment Fusion. <https://github.com/Netflix/vmaf.git>. Accessed: 2025-01-06.
- [Paszke et al.(2019)] Adam Paszke, Sam Gross, Francisco Massa, Adam Lerer, James Bradbury, Gregory Chanan, Trevor Killeen, Zeming Lin, Natalia Gimelshein, Luca Antiga, et al. 2019. PyTorch: An imperative style, high-performance deep learning library. *Advances in neural information processing systems* 32 (2019).
- [Smolak-Dyżewska et al.(2024)] Weronika Smolak-Dyżewska, Dawid Malarz, Kornel Howil, Jan Kaczmarczyk, Marcin Mazur, and Przemysław Spurek. 2024. VeGaS: Video Gaussian Splatting. *arXiv preprint arXiv:2411.11024* (2024).
- [Sullivan(2020)] Gary Sullivan. 2020. Versatile video coding (VVC) arrives. In *2020 IEEE International Conference on Visual Communications and Image Processing (VCIP)*. IEEE, 1–1.
- [Sullivan et al.(2012)] Gary J Sullivan, Jens-Rainer Ohm, Woo-Jin Han, and Thomas Wiegand. 2012. Overview of the high efficiency video coding (HEVC) standard. *IEEE Transactions on circuits and systems for video technology* 22, 12 (2012), 1649–1668.
- [Sun et al.(2024)] Yang-Tian Sun, Yi-Hua Huang, Lin Ma, Xiaoyang Lyu, Yan-Pei Cao, and Xiaojuan Qi. 2024. Splatter a Video: Video Gaussian Representation for Versatile Processing. *arXiv preprint arXiv:2406.13870* (2024).
- [Wang et al.(2003)] Zhou Wang, Eero P Simoncelli, and Alan C Bovik. 2003. Multiscale structural similarity for image quality assessment. In *The Thirty-Seventh Asilomar Conference on Signals, Systems & Computers, 2003*, Vol. 2. Ieee, 1398–1402.
- [Wiegand et al.(2003)] Thomas Wiegand, Gary J Sullivan, Gisle Bjontegaard, and Ajay Luthra. 2003. Overview of the H. 264/AVC video coding standard. *IEEE Transactions on circuits and systems for video technology* 13, 7 (2003), 560–576.
- [Xie et al.(2024)] Xingyu Xie, Pan Zhou, Huan Li, Zhouchen Lin, and Shuicheng Yan. 2024. Adan: Adaptive nesterov momentum algorithm for faster optimizing deep models. *IEEE Transactions on Pattern Analysis and Machine Intelligence* (2024).
- [Ye et al.(2024)] Vickie Ye, Ruilong Li, Justin Kerr, Matias Turkulainen, Brent Yi, Zhuoyang Pan, Otto Seiskari, Jianbo Ye, Jeffrey Hu, Matthew Tancik, and Angjoo Kanazawa. 2024. gsplat: An Open-Source Library for Gaussian Splatting. *arXiv preprint arXiv:2409.06765* (2024). arXiv:2409.06765 [cs.CV] <https://arxiv.org/abs/2409.06765>
- [Zeghidour et al.(2021)] Neil Zeghidour, Alejandro Luebs, Ahmed Omran, Jan Skoglund, and Marco Tagliasacchi. 2021. SoundStream: An end-to-end neural audio codec. *IEEE/ACM Transactions on Audio, Speech, and Language Processing* 30 (2021), 495–507.
- [Zhang et al.(2025)] Xinjie Zhang, Xingtong Ge, Tongda Xu, Dailan He, Yan Wang, Hongwei Qin, Guo Lu, Jing Geng, and Jun Zhang. 2025. GaussianImage: 1000 fps image representation and compression by 2d gaussian splatting. In *European Conference on Computer Vision*. Springer, 327–345.
- [Zhang et al.(2024)] Yunxiang Zhang, Alexandr Kuznetsov, Akshay Jindal, Kenneth Chen, Anton Sochenov, Anton Kaplanyan, and Qi Sun. 2024. Image-GS: Content-Adaptive Image Representation via 2D Gaussians. *arXiv preprint arXiv:2407.01866* (2024).